Oxidation of P700 in Photosystem I Is Essential for the Growth of Cyanobacteria

Shimakawa, Ginga
Shaku, Keiichiro
Miyake, Chikahiro

Oxidation of P700 in Photosystem I Is Essential for the Growth of Cyanobacteria[1][OPEN]

Ginga Shimakawa, Keiichiro Shaku, and Chikahiro Miyake*

Department of Biological and Environmental Science, Faculty of Agriculture, Graduate School of Agricultural Science, Kobe University, Nada-ku, Kobe 657–8501, Japan (G.S., K.S., C.M.); and Core Research for Environmental Science and Technology, Japan Science and Technology Agency, Chiyoda-ku, Tokyo 102–0076, Japan (C.M.)

ORCID ID: 0000-0002-2426-2377 (C.M.).

The photoinhibition of photosystem I (PSI) is lethal to oxygenic phototrophs. Nevertheless, it is unclear how photodamage occurs or how oxygenic phototrophs prevent it. Here, we provide evidence that keeping P700 (the reaction center chlorophyll in PSI) oxidized protects PSI. Previous studies have suggested that PSI photoinhibition does not occur in the two model cyanobacteria, *Synechocystis* sp. PCC 6803 and *Synechococcus elongatus* PCC 7942, when photosynthetic CO_2 fixation was suppressed under low CO_2 partial pressure even in mutants deficient in flavodiiron protein (FLV), which mediates alternative electron flow. The lack of FLV in *Synechococcus* sp. PCC 7002 (S. 7002), however, is linked directly to reduced growth and PSI photodamage under CO_2-limiting conditions. Unlike *Synechocystis* sp. PCC 6803 and *S. elongatus* PCC 7942, S. 7002 reduced P700 during CO_2-limited illumination in the absence of FLV, resulting in decreases in both PSI and photosynthetic activities. Even at normal air CO_2 concentration, the growth of S. 7002 mutant was retarded relative to that of the wild type. Therefore, P700 oxidation is essential for protecting PSI against photoinhibition. Here, we present various strategies to alleviate PSI photoinhibition in cyanobacteria.

Low CO_2 fixation efficiency in the Calvin-Benson cycle prevents the utilization of NADPH and ATP in photosynthesis and causes these molecules to accumulate, resulting in oxidative photosynthetic cell damage. High light, low temperature, and CO_2 limitation increase NADPH and ATP levels beyond the Calvin-Benson cycle requirements. Electrons and H^+ accumulate in the photosynthetic electron transport (PET) system. Excess electrons in the PET system trigger oxidative damage to PSI by forming reactive oxygen species (ROS), including the superoxide anion radical (O_2^-) and singlet oxygen ($^1O_2$), within PSI and degrading the P700 reaction center chlorophyll (P700; Sonoike, 1996; Sejima et al., 2014; Zivcak et al., 2015a, 2015b; Takagi et al., 2016). PSI repair has been reported to be a very slow process (Kudoh and Sonoike, 2002), and a recent study showed that it took more than 12 d for damaged PSI in wheat (*Triticum aestivum*) leaves to recover completely (Zivcak et al., 2015b). PSI photoinhibition, therefore, is very detrimental to oxygenic phototroph growth. Nevertheless, PSI photoinhibition is alleviated by keeping P700 oxidized (Sejima et al., 2014).

In the PET system of oxygenic phototrophs, P700 oxidation is a physiological response to environmental variations. In C_3 plants, low CO_2 and/or high light intensity induce P700 oxidation in vivo (Klughammer and Schreiber, 1994; Laisk and Oja, 1994; Miyake et al., 2004, 2005). Several molecular mechanisms are proposed for P700 oxidation wherein the PSI acceptor does not limit the PET reaction. First, H^+ accumulation on the lumenal side of thylakoid membranes lowers reduced plastoquinone (plastoquinol) oxidation rates in the cytochrome (Cyt) b_6/f complex (Kramer et al., 1999). Second, plastidial terminal oxidase and cyanobacterial respiratory terminal oxidases on the thylakoid membranes suppress PSI electron influx by accepting upstream PSI electrons in the PET system. Oxygen is the final electron acceptor (Beardall et al., 2003; Trouillard et al., 2012; Lea-Smith et al., 2013). Finally, plastoquinol accumulation inhibits the Q-cycle turnover in the Cyt b_6/f complex, which suppresses electron flow from the Cyt b_6/f complex to P700. This reaction is called the reduction-induced suppression of electron flow (RISE; Shaku et al., 2016). Overall, these molecular mechanisms contribute to P700 oxidation, thereby preventing PSI photoinhibition and enabling oxygenic phototrophs to thrive. The *proton gradient regulation5* (*pgr5*) mutant of Arabidopsis (*Arabidopsis thaliana*) cannot

[1] This work was supported by the Japan Society for the Promotion of Science (grant no. 26450079 to C.M. and research fellowship grant no. 16J03443 to G.S.) and by the Core Research for Evolutional Science and Technology of the Japan Science and Technology Agency (grant no. AL65D21010 to C.M.).

* Address correspondence to cmiyake@hawk.kobe-u.ac.jp.

The author responsible for distribution of materials integral to the findings presented in this article in accordance with the policy described in the Instructions for Authors (www.plantphysiol.org) is: Chikahiro Miyake (cmiyake@hawk.kobe-u.ac.jp).

C.M. conceived the original screening and research plans; C.M. supervised the experiments; G.S. performed most of the experiments; K.S. provided technical assistance to G.S.; C.M. and G.S. designed the experiments and analyzed the data; C.M. and G.S. conceived the project and wrote the article with contributions from all the authors; C.M. supervised and complemented the writing.

[OPEN] Articles can be viewed without a subscription.

www.plantphysiol.org/cgi/doi/10.1104/pp.16.01227

keep P700 oxidized and shows PSI photoinhibition under high-light and fluctuating light conditions (Munekage et al., 2002; Suorsa et al., 2012), which shows the importance of the oxidation of P700 for the protection of PSI in plants.

Unlike green plants, P700 oxidation mechanisms in cyanobacteria are unclear. It is known that flavodiiron protein (FLV) could contribute to P700 oxidation. Four FLV isozymes (FLV1−FLV4) have been identified in the model cyanobacterium *Synechocystis* sp. PCC 6803 (S. 6803; Helman et al., 2003). FLV1 and FLV3 (FLV1/3) function as a heterodimer and catalyze the reduction of oxygen to water on the acceptor side of PSI using NAD(P)H as electron donors (Vicente et al., 2002; Helman et al., 2003; Allahverdiyeva et al., 2013). Unlike FLV1/3, FLV2/4 is induced only under low CO_2 (Zhang et al., 2009) and mediates an oxygen-dependent alternative electron flow (AEF; Shimakawa et al., 2015). In S. 6803, FLV-dependent electron fluxes are coupled to photosynthesis and should alleviate electron overaccumulation in PSI (Helman et al., 2003, 2005; Allahverdiyeva et al., 2013; Shimakawa et al., 2015). Therefore, FLV is expected to contribute to P700 oxidation. The lack of FLV1/3 in S. 6803 causes PSI photoinhibition under artificial fluctuating light (Allahverdiyeva et al., 2013). However, under CO_2 limitation (which suppresses photosynthetic CO_2 fixation), deletions of FLV1/3 and FLV2/4 do not cause PSI photoinhibition in S. 6803 (Zhang et al., 2009) or *Synechococcus elongatus* PCC 7942 (S. 7942; Shaku et al., 2015), possibly because P700 stays oxidized under CO_2 limitation regardless of the existence of FLV (Shaku et al., 2015). These data imply that FLV is not essential to keep P700 oxidized under CO_2 limitation, at least in S. 6803 and S. 7942.

In this study, we found that the lack of FLV1/3 leads to growth inhibition under ambient [CO_2] concentration ([CO_2]) in the cyanobacterium *Synechococcus* sp. PCC 7002 (S. 7002), unlike S. 6803 and S. 7942 (Zhang et al., 2009; Shaku et al., 2015). The S. 7002 genome, like that of S. 7942, includes genes coding for FLV1/3 isozymes but not for FLV2/4 (Fujisawa et al., 2014). The genetic profiles of *flv* and other genes related to cyanobacterial AEF, including those of S. 7002, S. 6803, and S. 7942, are summarized in Table I. Shifting from CO_2-saturated to CO_2-limited conditions decreased total oxidizable P700 to approximately 10% in the *flv* knockout mutant of S. 7002 but not in those of S. 6803 or S. 7942. We demonstrated that the deletion of FLV in S. 7002 rendered it unable to oxidize P700, resulting in PSI photoinhibition. These findings show that there are different strategies in cyanobacteria to protect PSI against photooxidative damage under CO_2 limitation.

RESULTS

Effects of FLV on the Growth of S. 7002 under Ambient [CO_2]

We constructed the S. 7002 mutant, Δ*flv1/3*, which lacks the *flv1* and *flv3* orthologs present in S. 6803 (*SYNPCC7002_A1743* and *SYNPCC7002_A1321*; Supplemental Fig. S1). We found that the growth of S. 7002 Δ*flv1/3* is slower than that of the wild type under ambient [CO_2] (Fig. 1). This response was not observed in either S. 6803 (Zhang et al., 2009) or S. 7942 (Shaku et al., 2015). Approximately 2 weeks after inoculation, the OD_{750} for Δ*flv1/3* was 70% lower than that for the wild type (Fig. 1A). The chlorophyll (Chl) content in the Δ*flv1/3* medium was half that of the wild type (Fig. 1B). These results indicate that S. 7002 requires FLV1/3 for optimal growth under ambient [CO_2].

Effects of CO_2 Limitation on Photosynthetic Parameters in Wild-Type and Δ*flv1/3* S. 7002

We hypothesized that PSI photoinhibition occurs under CO_2 limitation in the absence of FLV-mediated AEF in S. 7002. We studied the effects of CO_2 limitation on total oxidizable P700 and net photosynthetic oxygen evolution rates in S. 7002 wild type and Δ*flv1/3*. After a 2-h exposure to CO_2 limitation, neither PSI nor photosynthesis inactivation was detected in S. 7002 wild type (Fig. 2, A and B). Nevertheless, a significant posttreatment reduction in total oxidizable P700 (Fig. 2A) and suppression of photosynthesis (Fig. 2C) were observed in S. 7002 Δ*flv1/3*. The dramatic decreases in photosynthetic parameters (0%−10% of pretreatment levels; Fig. 2, A and C) for Δ*flv1/3* indicate that the lack of FLV1/3 in S. 7002 causes severe PSI photoinhibition under CO_2 limitation.

To determine whether the deletion of FLV-mediated AEF combined with CO_2 limitation always causes PSI photoinhibition in cyanobacteria, we applied the same treatment to S. 6803 and S. 7942. For S. 6803, we used a

Table I. *Genetic background of AEF in three cyanobacteria species used in this study*

Gene homology analyses were performed in Cyanobase (http://genome.microbedb.jp/CyanoBase; Fujisawa et al., 2014). *cox*, aa_3-type cytochrome *c* oxidase; *cyd*, cytochrome *bd*-type quinol oxidase; *arto*, cytochrome b_o-type quinol oxidase; *ndhD*, D subunit of NAD(P)H dehydrogenase.

Cyanobacteria	Flavodiiron Proteins		Respiratory Terminal Oxidases			Cyclic Electron Flow	
	flv1/3	*flv2/4*	*cox*	*cyd*	*arto*	*ndhD1/2*	*pgr5*
S. 7002 (*SYNPCC7002_*)	*A1743/A1321*	−	*A1162 −A1164*	−	*A0725 −A0727*	*A2000/A1973*	*A1477*
S. 6803	*sll1521/sll0550*	*sll0219/sll0217*	*slr1136 −slr1138*	*slr1379/slr1380*	*slr2082/slr2083/sll0813*	*slr0331/slr1291*	*ssr2016*
S. 7942 (*SYNPCC7942_*)	*1810/1809*	−	*2602 −2604*	*1766/1767*	−	*1976/1439*	−

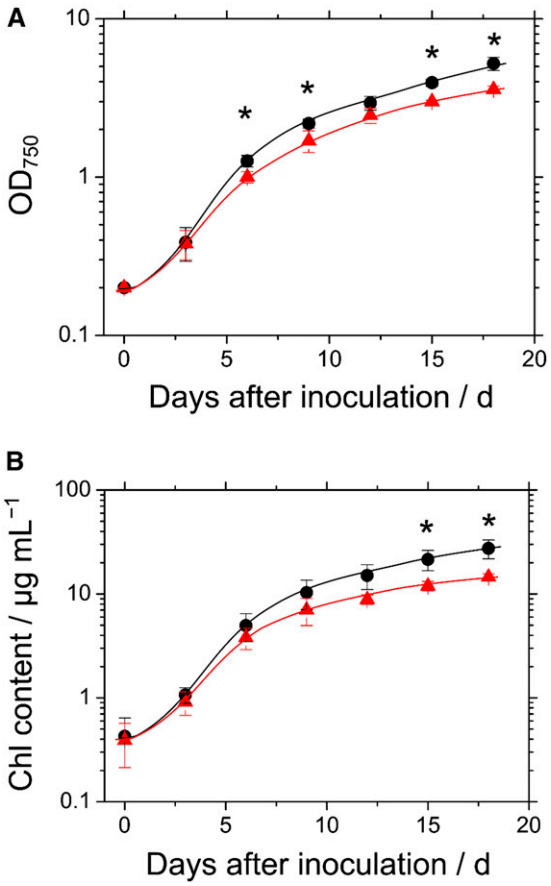

Figure 1. Growth of S. 7002 wild type and the mutant Δ*flv1/3* under ambient [CO_2]. Optical density at 750 nm (OD_{750}; A) and Chl (B) measurements were independently conducted three times, and the data are shown as means ± SD. Black circles, S. 7002 wild type; red triangles, Δ*flv1/3*. Differences between S. 7002 wild type and Δ*flv1/3* were analyzed by Student's *t* test. Asterisks indicate statistically significant differences between S. 7002 wild type and Δ*flv1/3* at $P < 0.05$.

mutant deficient in the expression of all four *flv* genes (Δ*flv1/3/4*), since the wild type of this species possesses FLV2/4 (Table I; Supplemental Fig. S1; Eisenhut et al., 2012). Unlike S. 7002, the amounts of total oxidizable P700 were the same before and after the treatment for both S. 6803 and S. 7942 even when the *flv* genes were not expressed (Supplemental Fig. S2, A and B). CO_2 limitation also did not affect the dependence of photosynthetic oxygen evolution rates on photon flux density in either the wild type or the *flv* mutants of S. 6803 and S. 7942 (Supplemental Fig. S2, C–F). On the other hand, the deletion of FLV1/3 in S. 7942 decreased photosynthetic oxygen evolution rates even before CO_2 limitation, particularly in high-light conditions (Supplemental Fig. S2, D and F), due to RISE (Shaku et al., 2015).

Effects of FLV on the Photosynthetic Parameters of PSII and PSI in S. 7002

To determine the relationship between PSI photodamage and P700 oxidation in S. 7002, we simultaneously monitored Chl fluorescence and the P700 redox state in PSI during the transition from CO_2 saturation to CO_2 limitation. We modified methods used in our previous

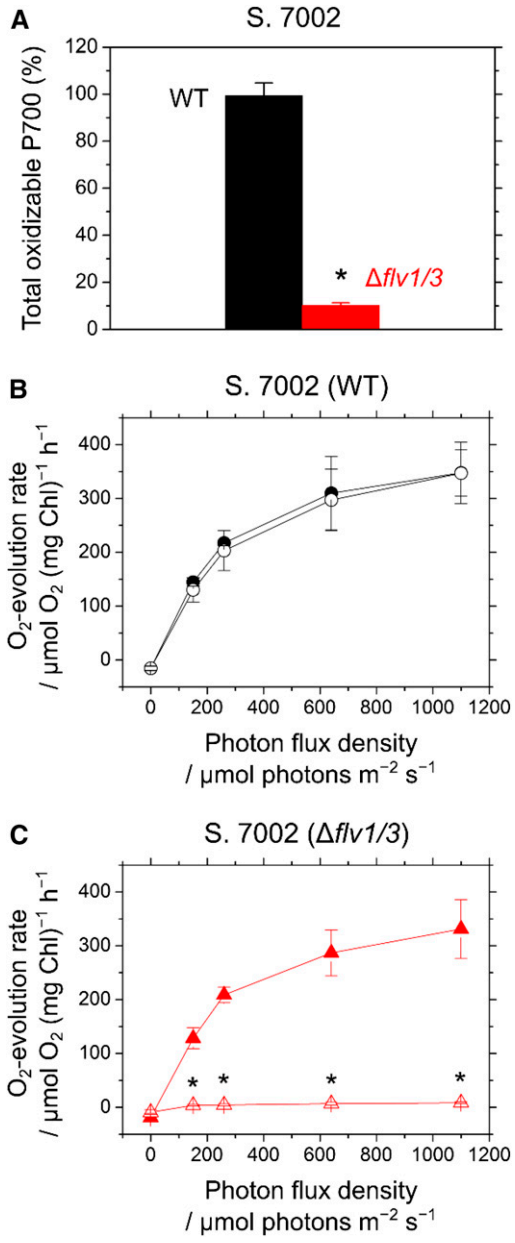

Figure 2. Reduced activities of PSI and photosynthesis in S. 7002 wild type (WT) and Δ*flv1/3* after 2-h exposures to CO_2 limitation during illumination (290 μmol photons m^{-2} s^{-1}). The reaction mixture contained fresh A^+ medium and cyanobacterial cells (10 μg Chl mL^{-1}). Residual total oxidizable P700 (A) and photosynthetic oxygen evolution rates (B and C) were measured before and after 1 h in the dark following treatments. Black and red symbols represent the wild type and Δ*flv1/3*, respectively. Closed and open symbols represent the data before and after the treatments (B and C), respectively. Photosynthetic oxygen evolution rates were measured in the presence of 10 mM $NaHCO_3$. Each measurement was conducted three times, and means ± SD are shown. Differences between the data before and after the treatments were analyzed by Student's *t* test. Asterisks indicate statistically significant differences at $P < 0.05$.

work (Shimakawa et al., 2015). Upon red actinic light (AL) illumination in S. 7002 wild type, incident quantum yields of PSI [Y(I)] and PSII [Y(II)] rose (by about 0.8 and 0.3, respectively). Thereafter, they began to decline (to about 0.6 and 0.1, respectively) due to a decrease in photosynthesis (Fig. 3A). CO_2 consumption suppressed photosynthesis. Y(I) and Y(II) were restored when CO_2 was added in the form of $NaHCO_3$ (Fig. 3A; Hayashi et al., 2014; Shimakawa et al., 2015). The P700 redox state also responded to CO_2 limitation. The suppression of photosynthetic linear electron flow increased the yield of oxidized P700 [Y(ND)]. This condition was alleviated by the addition of CO_2 (Fig. 3A). On the other hand, the yield of photoexcited P700 [Y(NA)] did not change in response to the shortage of CO_2 (Fig. 3A). Therefore, the PSI acceptor side limitation did not change after S. 7002 wild type was subjected to CO_2 limitation. It is unclear why Y(I) was significantly higher than Y(II) in this study. Cyclic electron flow around PSI may contribute to surplus Y(I) (see "Discussion"). The S. 6803 mutant Δ*ndhD1/2*, which is deficient in the D subunits of NAD(P)H dehydrogenase, however, also had higher Y(I) than Y(II) (Supplemental Fig. S3). The large gap between Y(I) and Y(II) in cyanobacteria merits further investigation.

Next, we measured the photosynthetic parameters of PSII and PSI after the transition to CO_2 limitation in S. 7002 Δ*flv1/3*. Before CO_2 deprivation, Y(I) and Y(II) in Δ*flv1/3* were lower (about 0.6 and 0.2, respectively) than those in the wild type, whereas Y(NA) was higher in the mutant (about 0.3) than in the wild type (about 0.1; Fig. 3). These results imply that FLV1/3 drives AEF in S. 7002, as it does for S. 6803 (Helman et al., 2003) and S. 7942 (Shaku et al., 2015). CO_2 limitation did not induce P700 oxidation in S. 7002 Δ*flv1/3* (Fig. 3B). An increase in Y(NA) indicated that the electron flux from P700 to the acceptor side of PSI was reduced further still (Fig. 3B). Y(I) also was considerably suppressed under CO_2 limitation (Fig. 3B). The addition of $NaHCO_3$ did not restore Y(I) or Y(II) (Fig. 3B). These results suggest that, unless FLV1/3-mediated AEF is active, PSI photoinhibition occurs in S. 7002 during CO_2 limitation. For S. 7002, FLV1/3 plays a primary role in oxidizing the PET system under CO_2 limitation. Recently, we found that S. 7002 drives an oxygen-dependent AEF to restore linear electron transport during CO_2-limited photosynthesis. This process is particularly evident in cells grown under ambient [CO_2] (Shimakawa et al., 2016). In this study, a simultaneous measurement of oxygen concentration and Chl fluorescence was performed in S. 7002 Δ*flv1/3* grown under ambient [CO_2] (Supplemental Fig. S4), indicating that FLV1/3 is the molecular mechanism of the oxygen-dependent AEF we found in S. 7002 (Shimakawa et al., 2016).

Effects of FLV on the Photosynthetic Parameters of PSII and PSI in S. 6803 and S. 7942

The photosynthetic parameters of PSII and PSI responded differently to CO_2 limitation in S. 6803 than they did in S. 7002. In S. 6803 wild type, Y(I) and Y(II)

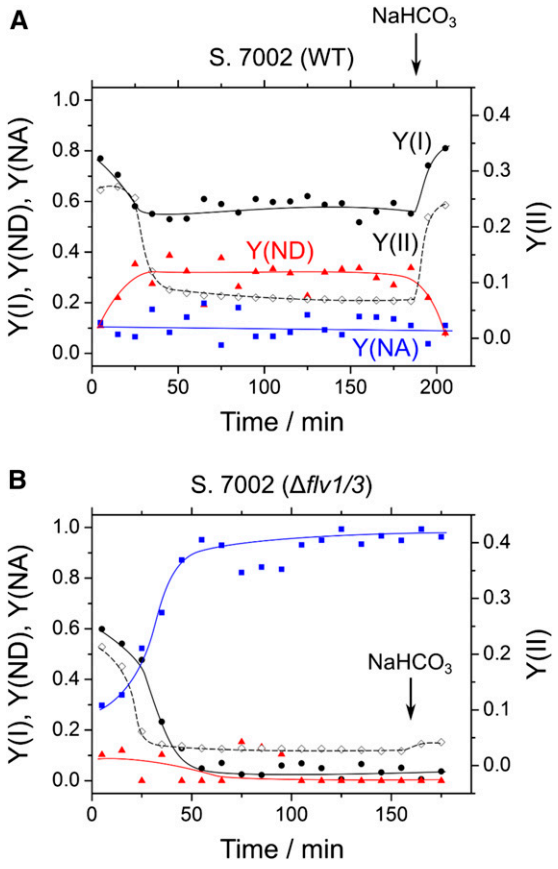

Figure 3. Responses of the photosynthetic parameters of PSII and PSI to CO_2 limitation in S. 7002 wild type (WT; A) and the mutant Δ*flv1/3* (B). Reaction mixtures contained the cells (10 μg Chl mL^{-1}). Black circles, Y(I); red triangles, Y(ND); blue squares, Y(NA); white diamonds, Y(II). Red AL (180 μmol photons m^{-2} s^{-1}) was activated at time zero. $NaHCO_3$ (10 mM) was added as indicated. Measurements were conducted three times, and representative data are shown.

decreased to minimum values and then started to recover, reaching approximately 90% and 60% of the initial values, respectively, without the addition of $NaHCO_3$ (Supplemental Fig. S5A). This recovery occurred due to the activation of an oxygen-dependent AEF driven by FLV2/4 but not by FLV1/3 (Shimakawa et al., 2015; Supplemental Figs. S5 and S6). The AEF stimulated linear electron flow, which decreased both Y(ND) and Y(NA) (Supplemental Fig. S5A). In S. 6803, the deletion of FLV1/3 reduced both Y(I) and Y(II) relative to the wild type before CO_2 consumption (Supplemental Fig. S5B). For S. 6803 Δ*flv1/3* before CO_2 depletion, Y(ND) was lower than that of the S. 6803 wild type, whereas Y(NA) in the mutant was higher than that of the wild type (Supplemental Fig. S5B). These findings concur with those of previous studies showing that FLV1/3-mediated AEF can oxidize P700 (Helman et al., 2003; Allahverdiyeva et al., 2013; Hayashi et al., 2014). The suppression of photosynthetic linear electron flow caused by CO_2 limitation induced P700 oxidation in S. 6803 even in the absence of

FLV-mediated electron flow (Supplemental Fig. S5D). The oxidized P700 was reduced by the activation of FLV2/4-mediated AEF or by the resumption of photosynthetic CO_2 fixation (Supplemental Fig. S5).

S. 7942 wild type lacks FLV2/4-mediated AEF (Hayashi et al., 2014), so its PSII and PSI photosynthetic parameters responded to CO_2 limitation in almost the same manner as did those of S. 6803 Δ*flv4*. For the S. 7942 wild type, both Y(I) and Y(II) decreased and remained low under CO_2 limitation, but they were restored by adding $NaHCO_3$ (Supplemental Fig. S7A). The increase in Y(ND) reflected P700 oxidation in response to CO_2 limitation and was observed in both the wild type and Δ*flv1/3* of S. 7942 (Supplemental Fig. S7). The mutant of S. 7942 also had a higher Y(ND) than did the S. 7942 wild type under CO_2 limitation (Supplemental Fig. S7B). These results align with the findings of a previous study (Shaku et al., 2015).

DISCUSSION

Table II summarizes the findings of previous studies and this study and shows two main conclusions: (1) P700 oxidation is linked directly to the protection of PSI against photoinhibition; and (2) in cyanobacteria, there are several strategies, including FLV, to alleviate PSI photoinhibition. In S. 7002, FLV1/3 mediates oxygen-dependent AEF that regulates the PSI redox state and promotes P700 oxidation under CO_2 limitation (Fig. 3; Supplemental Fig. S4; Shimakawa et al., 2016). In S. 7002, the lack of FLV-mediated AEF resulted in P700 reduction, photosynthesis suppression, PSI photoinhibition, and growth retardation (Figs. 1 and 2). These observations correspond to higher transcript levels of *flv1/3* under CO_2 limitation (Ludwig and Bryant, 2012). In contrast, S. 6803 and S. 7942 keep P700 oxidized under CO_2 limitation independently of FLV-mediated AEF (which protects PSI against photooxidative damage; Supplemental Figs. S2, S5, and S7; Zhang et al., 2009; Shaku et al., 2015). In cyanobacteria, FLV has diverse physiological significance as the agent for oxygen-dependent AEF.

In this study, we showed that P700 oxidation protects PSI against photoinhibition in cyanobacteria (which are the progenitors of oxygenic phototrophs). Photooxidative damage in PSI is caused by ROS generated by excitation energy transfer from P700 ultimately to oxygen. Therefore, photooxidizable P700 in PSI can produce ROS, whereas oxidized P700 cannot be excited by photon energy. PSI photoinhibition is caused by O_2^- produced on the acceptor side of PSI when $NADP^+$ regeneration is limited (Hihara and Sonoike, 2001). Added hydrogen peroxide reacts with reduced iron in iron-sulfur centers to form hydroxyl radicals that destroy PSI instantaneously (Hihara and Sonoike, 2001; Sonoike, 2011). P700 oxidation is expected to negate the effect of hydroxyl radicals by suppressing O_2^- generation and by oxidizing the iron-sulfur centers (Sonoike 1996). Recently, it was suggested that $^1O_2$ triggers PSI photoinhibition (Cazzaniga et al., 2012, 2016; Takagi et al., 2016). Keeping P700 oxidized should help suppress $^1O_2$ generation. P700 oxidation alleviates PSI photoinhibition in sunflower (*Helianthus annuus*) leaves during repetitive short saturated-pulse treatment (Sejima et al., 2014). There may be a mechanism common both to plants and cyanobacteria for protecting PSI from photooxidative damage. P700 oxidation would be a hedge against ROS generation.

In S. 6803 and S. 7942, P700 remained oxidized under CO_2 limitation even without FLV1/3 and FLV2/4 (Supplemental Figs. S5 and S7). There is, therefore, a P700 oxidation mechanism that operates independently of FLV-mediated AEF under CO_2 limitation. One candidate is cyclic electron flow around PSI, which helps induce the proton gradient across the thylakoid membrane (Miyake et al., 2004, 2005). Acidification of the lumenal side reduces the oxidation activity of plastoquinol in the Cyt b_6/f complex and limits the electron flux from plastoquinol to P700 through plastocyanin (or Cyt *c*). These hypotheses are supported by the fact that Y(I) is greater than Y(II) for all cyanobacterial strains tested except for S. 7002 Δ*flv1/3* (Fig. 3; Supplemental Figs. S5 and S7). Nevertheless, we also found that Y(I) is greater than Y(II) for both S. 6803 wild type and its mutant Δ*ndhD1/2* (Supplemental Fig. S3). Therefore, reduced activity of NAD(P)H dehydrogenase-mediated cyclic electron flow (Ohkawa et al., 2000) is not linked to the ratio of Y(I) to Y(II). Moreover, cyclic electron transport rates in S. 6803 and S. 7002 are negligible relative to their photosynthetic linear and

Table II. *Phenotypes of each wild type and* flv *mutant under CO_2 limitation in three cyanobacteria species used in this study*

Cyanobacteria	Type	Growth	Y(II)	Y(I)	P700 Redox	PSI
S. 7002	Wild type	Well	High[a]	High[a]	Oxidized	Safe
	Δ*flv1/3*	Bad	Low	Low	Reduced	Broken
S. 6803	Wild type	Well	High[b]	High	Oxidized	Safe
	Δ*flv1/3*	Well[c]	High[b]	High	Oxidized	Safe
	Δ*flv4*	Bad[c]	Low[d]	Low	Oxidized	Safe[c]
	Δ*flv1/3/4*	−	Low	Low	Oxidized	Safe
S. 7942	Wild type	Well	Low[b]	Low[e]	Oxidized[e]	Safe[e]
	Δ*flv1/3*	Well[e]	Low[e]	Low[e]	Oxidized[e]	Safe[e]

[a]Shimakawa et al. (2016). [b]Hayashi et al. (2014). [c]Zhang et al. (2009). [d]Shimakawa et al. (2015). [e]Shaku et al. (2016).

respiratory electron transport rates (Yu et al., 1993; Shimakawa et al., 2014). We could not determine why Y(I) differed from Y(II) in cyanobacteria. The contribution of phycobiliprotein to minimum fluorescence yield may account for it (Campbell et al., 1998), as might the difference between the quality of the growth light and that of the light-emitting diode (LED)-sourced AL used in the experiments. Another candidate for the P700 oxidation mechanism is the suppression of the Q cycle when plastoquinone is reduced. In this case, the electron flux from the Cyt b_6/f complex to P700 in PSI decreases. This response is called RISE (Shaku et al., 2015), and it might be the main driver of P700 oxidation under CO_2 limitation in cyanobacteria. Respiratory terminal oxidases like Cyt *c* oxidase and cytochrome *bd*-type quinol oxidase also may contribute to the oxidation of the donor side of PSI under CO_2 limitation (Beardall et al., 2003; Trouillard et al., 2012; Lea-Smith et al., 2013). It is difficult, however, to explain why Y(II) decreased during CO_2 limitation in the cyanobacteria we studied (Fig. 3; Supplemental Figs. S5 and S7).

In S. 6803, FLV2/4 may receive electrons from the acceptor side of PSI. In both S. 6803 wild type and its mutant Δ*flv1/3*, the increases in Y(I) and Y(II) indicate that PSI electron flux is restored under CO_2 limitation (Supplemental Fig. S5, A and B). Unlike S. 6803 wild type and Δ*flv1/3*, neither Δ*flv4* nor Δ*flv1/3/4* experienced an increase in Y(I) (Supplemental Fig. S5, C and D). Removing oxygen lowered Y(I) under CO_2 limitation in S. 6803 wild type but not in Δ*flv4* (Supplemental Fig. S6). These data suggest that FLV2/4 mediates an oxygen-dependent AEF on the acceptor side of PSI (Hayashi et al., 2014; Shimakawa et al., 2015), as does FLV1/3 (Helman et al., 2003), since both FLV sets have similar primary structures (Fujisawa et al., 2014) and enzymatic characteristics of recombinant proteins (Vicente et al., 2002; Shimakawa et al., 2015). However, we cannot exclude the possibility that the relief of excitation pressure at PSII by FLV2/4 (Bersanini et al., 2014) provides an enhancement of Y(I) during CO_2-limited photosynthesis in S. 6803. FLV2/4 is known to interact with PSII and phycobilisomes (Bersanini et al., 2014), so in S. 6803, it may have multiple functions to alleviate photoinhibition under low CO_2.

MATERIALS AND METHODS

Growth Conditions and Chl *a* Determination

Cyanobacterial cultures were maintained under continuous fluorescent lighting (25°C, 50 μmol photons m^{-2} s^{-1}) on BG-11 solid medium (for *Synechocystis* sp. PCC 6803 and *Synechococcus elongatus* PCC 7942) and A^+ solid medium (for *Synechococcus* sp. PCC 7002; Allen, 1968; Stevens and Porter, 1980). Cells from both cultures were inoculated into liquid medium (initial OD_{750} = 0.1–0.2) and grown on a rotary shaker (100 rpm) under continuous fluorescent lighting (25°C, 150 μmol photons m^{-2} s^{-1}) at 2,000 μL L^{-1} [CO_2]. OD_{750} values were measured with a spectrophotometer (U-2800A; Hitachi). For all photosynthetic parameter measurements, cells from the exponential growth phase were used. In the experiments for Figure 1 and Supplemental Figure S4, S. 7002 was grown under ambient [CO_2].

For Chl measurements, cells from 0.1- to 1-mL cultures were centrifugally harvested and resuspended by vortexing in 1 mL of 100% (v/v) methanol. After incubation at room temperature for 5 min, the suspension was centrifuged at 10,000*g* for 5 min. Total Chl *a* was spectrophotometrically determined from the supernatant (Grimme and Boardman, 1972).

Bioinformatics

All the S. 7002, S. 6803, and S. 7942 gene sequence data used in this study were obtained from Cyanobase (http://genome.microbedb.jp/CyanoBase; Fujisawa et al., 2014). For the *flv1−4*, *cox*, *cyd*, *arto*, *ndhD1/2*, and *pgr5* gene sequences, BLAST searches were conducted in Cyanobase.

Statistical Analysis

Student's *t* tests were applied to detect differences. All statistical analyses were performed using Microsoft Excel 2010 (Microsoft) and JMP8 (SAS Institute).

Generation of Mutants

The triple mutant of S. 6803 deficient in *flv1* (*sll1521*), *flv3* (*sll0550*), and *flv4* (*sll0217*) was generated by transforming Δ*flv1/3* (Hayashi et al., 2014) using the *flv4* construct (Shimakawa et al., 2015). PCR was used to confirm the complete segregation of *flv1* and *flv4* (Supplemental Fig. S1A). The disruption of FLV3 proteins was verified by immunoblotting with a specific antibody to FLV3 (see "Immunoblot Analysis" below), since a nonspecific band was observed near the target band in the PCR analysis (Supplemental Fig. S1B).

To construct the double mutant of S. 7002 lacking *flv1* (*SYNPCC7002_A1743*) and *flv3* (*SYNPCC7002_A1321*) orthologs, PCR was used to amplify each genomic region encoding *A1743* and *A1321* with the up f and dn r primer sets (Supplemental Table S1). They were then cloned into the pGEM-T Easy vector (Promega). The recombinant plasmids containing *A1743* and *A1321* were linearized and amplified by inverse PCR with the up f and dn r primer sets (Supplemental Table S1). They were then applied to the In-Fusion reaction (Takara) using chloramphenicol and kanamycin resistance genes (Cm^r and Kan^r) derived from pACYC184 and pUC4K vectors, respectively (Rose, 1988; Taylor and Rose, 1988). Transformation of S. 7002 was performed by the standard procedure (Frigaard et al., 2004). Single mutants (Δ*flv1* and Δ*flv3*) were selected on 0.5% BG-11 agar plates containing chloramphenicol (15 μg mL^{-1}) or kanamycin (50 μg mL^{-1}). The double mutant (Δ*flv1/3*) was generated by transforming Δ*flv1* with the Δ*flv3* construct. The mutants were selected on plates containing both chloramphenicol (15 μg mL^{-1}) and kanamycin (50 μg mL^{-1}). Complete segregation was confirmed by PCR (Supplemental Fig. S1C).

Immunoblot Analysis

S. 6803 wild-type and Δ*flv1/3/4* cell cultures (10 mL) were harvested by centrifugation and pellet resuspension in 500 μL of extraction buffer (50 mM HEPES-KOH [pH 7.5], 1 mM $MgCl_2$, 2 mM EDTA, and 1 mM phenylmethylsulfonyl fluoride). The suspensions were homogenized with glass beads using Bug Crasher GM-01 (Taitec) and centrifuged at 13,000*g* for 30 min at 4°C. The supernatants were treated as extracted soluble fractions. Protein concentrations in them were determined with the Pierce 660 nm Protein Assay (Thermo Scientific) using bovine serum albumin as the standard. Soluble fractions containing 5 μg of protein were analyzed by SDS-PAGE. After electrophoresis, the proteins were electrotransferred to a polyvinylidene fluoride membrane and detected by an FLV3-specific antibody (kindly provided by Dr. H. Yamamoto).

Measurement of Chl Fluorescence and P700

Chl fluorescence and P700 were measured simultaneously with the Dual-PAM-100 system (Heinz Walz) at room temperature (25°C ± 2°C). For S. 6803 and S. 7942, the reaction mixtures (2 mL) contained 50 mM HEPES (pH 7.5) and the cells (10 μg Chl mL^{-1}). For S. 7002, the reaction mixture consisted of fresh A^+ medium and the cells (10 μg Chl mL^{-1}). During the measurements, the reaction mixtures were stirred with a magnetic micro stirrer. The photon flux densities of red AL (LED with peak emission at 635 nm) are shown in the corresponding figure legends. Y(II) reflects the apparent electron flux in photosynthetic linear electron transport (Genty et al., 1989). It was calculated from Chl fluorescence as $(F_m' - F_s)/F_m'$ (where F_m' = maximum variable fluorescence yield, F_s = steady-state fluorescence yield, and F_o = minimum fluorescence yield; Schreiber et al.,

1986; van Kooten and Snel, 1990). The redox state of P700 was determined according to the method of Klughammer and Schreiber (1994, 2008). In this procedure, P_m = the maximum P700 photooxidation level obtained by saturated pulse light under far-red illumination, P = the oxidation level of P700 under AL, P_m' = maximum oxidation level of P700 obtained by saturation pulse under AL illumination, Y(I) = $(P_m' - P)/P_m$ = the incident quantum yield of photochemical energy conversion, Y(ND) = P/P_m = the quantum yield of nonphotochemical energy dissipation due to donor-side limitation, and Y(NA) = $(P_m - P_m')/P_m$ = the quantum yield of nonphotochemical energy dissipation due to acceptor-side limitation. The sum of the three factors [Y(I) + Y(NA) + Y(ND)] = 1. For the simultaneous measurements of Y(II), Y(I), Y(ND), and Y(NA), a 300-ms saturation pulse (10,000 μmol photons m^{-2} s^{-1}) was supplied every 10 min. The stirrer was turned off 5 s before the saturation pulse was applied.

Measurement of Oxygen Exchange

Oxygen uptake and evolution were measured with a Clark-type oxygen electrode (Hansatech; Shimakawa et al., 2015). For S. 6803 and S. 7942, the reaction mixture (2 mL) contained 50 mM HEPES (pH 7.5), 10 mM $NaHCO_3$, and the cells (10 μg Chl mL^{-1}). For S. 7002, the mixture (2 mL) contained fresh A^+ medium, 10 mM $NaHCO_3$, and the cells (10 μg Chl mL^{-1}). Cells were illuminated with AL (red light, 620 < wavelength < 695 nm; photon flux densities are indicated in the figure legends) at 25°C. During the measurements, the reaction mixture was stirred with a magnetic micro stirrer.

Oxygen concentration and Chl fluorescence were measured simultaneously (Supplemental Fig. S4). The relative fluorescence of Chl *a* was measured with a Chl fluorometer (PAM-101; Heinz Walz; Schreiber et al., 1986; Shimakawa et al., 2015). Pulse-modulated excitation was achieved using an LED lamp with peak emission at 650 nm. Modulated fluorescence was measured at $\lambda > 710$ nm using a Schott RG9 long-pass filter. The fluorescence terminology follows van Kooten and Snel (1990).

Supplemental Data

The following supplemental materials are available.

Supplemental Figure S1. Insertional inactivation of *flv* genes in S. 6803 and S. 7002.

Supplemental Figure S2. Decreased activities of PSI and photosynthesis in the wild type and the *flv* mutants of S. 6803 and S. 7942 after 2-h exposures to CO_2 limitation during illumination.

Supplemental Figure S3. Responses of the photosynthetic parameters of PSII and PSI to CO_2 limitation in the mutant of S. 6803 deficient in *ndhD1* and *ndhD2*.

Supplemental Figure S4. Photosynthetic parameters of S. 7002 wild type and Δ*flv1/3* grown in ambient [CO_2].

Supplemental Figure S5. Responses of the photosynthetic parameters of PSII and PSI to CO_2 limitation in S. 6803 wild type and the mutants Δ*flv1/3*, Δ*flv4*, and Δ*flv1/3/4*.

Supplemental Figure S6. Effects of eliminating oxygen on the photosynthetic parameters of PSII and PSI under CO_2 limitation in S. 6803 wild type and the mutant Δ*flv4*.

Supplemental Figure S7. Responses of the photosynthetic parameters of PSII and PSI to CO_2 limitation in S. 7942 wild type and the mutant Δ*flv1/3*.

Supplemental Table S1. Primers used in this study.

ACKNOWLEDGMENTS

We thank Akihiko Kondo, Tomohisa Hasunuma, and Dr. Shimpei Aikawa (Kobe University) for supplying the S. 7002 wild type; Dr. Hiroshi Ohkawa (Hirosaki University) and Kintake Sonoike (Waseda University) for giving us the mutant Δ*ndhD1/2*; Dr. Hiroshi Yamamoto (Kyoto University) for the gift of the anti-FLV3 antibody; and Editage (www.editage.jp) for English language editing.

Received August 4, 2016; accepted September 7, 2016; published September 9, 2016.

LITERATURE CITED

Allahverdiyeva Y, Mustila H, Ermakova M, Bersanini L, Richaud P, Ajlani G, Battchikova N, Cournac L, Aro EM (2013) Flavodiiron proteins Flv1 and Flv3 enable cyanobacterial growth and photosynthesis under fluctuating light. Proc Natl Acad Sci USA **110:** 4111–4116

Allen MM (1968) Simple conditions for growth of unicellular blue-green algae on plates1, 2. J Phycol **4:** 1–4

Beardall J, Quigg A, Raven JA (2003) Oxygen consumption: photorespiration and chlororespiration. *In* WD Larkum, SE Douglas, JA Raven, eds, Photosynthesis in Algae. Kluwer Academic Publishers, Dordrecht, The Netherlands, pp 157–181

Bersanini L, Battchikova N, Jokel M, Rehman A, Vass I, Allahverdiyeva Y, Aro EM (2014) Flavodiiron protein Flv2/Flv4-related photoprotective mechanism dissipates excitation pressure of PSII in cooperation with phycobilisomes in cyanobacteria. Plant Physiol **164:** 805–818

Campbell D, Hurry V, Clarke AK, Gustafsson P, Öquist G (1998) Chlorophyll fluorescence analysis of cyanobacterial photosynthesis and acclimation. Microbiol Mol Biol Rev **62:** 667–683

Cazzaniga S, Bressan M, Carbonera D, Agostini A, Dall'Osto L (2016) Differential roles of carotenes and xanthophylls in photosystem I photoprotection. Biochemistry **55:** 3636–3649

Cazzaniga S, Li Z, Niyogi KK, Bassi R, Dall'Osto L (2012) The Arabidopsis *szl1* mutant reveals a critical role of β-carotene in photosystem I photoprotection. Plant Physiol **159:** 1745–1758

Eisenhut M, Georg J, Klähn S, Sakurai I, Mustila H, Zhang P, Hess WR, Aro EM (2012) The antisense RNA As1_flv4 in the cyanobacterium *Synechocystis* sp. PCC 6803 prevents premature expression of the *flv4-2* operon upon shift in inorganic carbon supply. J Biol Chem **287:** 33153–33162

Frigaard NU, Sakuragi Y, Bryant DA (2004) Gene inactivation in the cyanobacterium *Synechococcus* sp. PCC 7002 and the green sulfur bacterium *Chlorobium tepidum* using in vitro-made DNA constructs and natural transformation. *In* R Carpentier, ed, Photosynthesis Research Protocols. Humana, Totowa, NJ, pp 325–340

Fujisawa T, Okamoto S, Katayama T, Nakao M, Yoshimura H, Kajiya-Kanegae H, Yamamoto S, Yano C, Yanaka Y, Maita H, et al (2014) CyanoBase and RhizoBase: databases of manually curated annotations for cyanobacterial and rhizobial genomes. Nucleic Acids Res **42:** D666–D670

Genty B, Briantais JM, Baker NR (1989) The relationship between the quantum yield of photosynthetic electron transport and quenching of chlorophyll fluorescence. Biochim Biophys Acta **990:** 87–92

Grimme LH, Boardman NK (1972) Photochemical activities of a particle fraction P 1 obtained from the green alga Chlorella fusca. Biochem Biophys Res Commun **49:** 1617–1623

Hayashi R, Shimakawa G, Shaku K, Shimizu S, Akimoto S, Yamamoto H, Amako K, Sugimoto T, Tamoi M, Makino A, et al (2014) O_2-dependent large electron flow functioned as an electron sink, replacing the steady-state electron flux in photosynthesis in the cyanobacterium *Synechocystis* sp. PCC 6803, but not in the cyanobacterium *Synechococcus* sp. PCC 7942. Biosci Biotechnol Biochem **78:** 384–393

Helman Y, Barkan E, Eisenstadt D, Luz B, Kaplan A (2005) Fractionation of the three stable oxygen isotopes by oxygen-producing and oxygen-consuming reactions in photosynthetic organisms. Plant Physiol **138:** 2292–2298

Helman Y, Tchernov D, Reinhold L, Shibata M, Ogawa T, Schwarz R, Ohad I, Kaplan A (2003) Genes encoding A-type flavoproteins are essential for photoreduction of O_2 in cyanobacteria. Curr Biol **13:** 230–235

Hihara Y, Sonoike K (2001) Regulation, inhibition and protection of photosystem I. *In* EM Aro, B Andersson, eds, Regulation of Photosynthesis. Kluwer Academic Publishers, Dordrecht, The Netherlands, pp 507–531

Klughammer C, Schreiber U (1994) An improved method, using saturating light pulses, for the determination of photosystem I quantum yield via $P700^+$-absorbance changes at 830 nm. Planta **192:** 261–268

Klughammer C, Schreiber U (2008) Saturation pulse method for assessment of energy conversion in PSI. PAM Application Notes **1:** 11–14

Kramer DM, Sacksteder CA, Cruz JA (1999) How acidic is the lumen? Photosynth Res **60:** 151–163

Kudoh H, Sonoike K (2002) Irreversible damage to photosystem I by chilling in the light: cause of the degradation of chlorophyll after returning to normal growth temperature. Planta **215:** 541–548

Laisk A, Oja V (1994) Range of photosynthetic control of postillumination $P700^+$ reduction rate in sunflower leaves. Photosynth Res **39:** 39–50

Lea-Smith DJ, Ross N, Zori M, Bendall DS, Dennis JS, Scott SA, Smith AG, Howe CJ (2013) Thylakoid terminal oxidases are essential for the cyanobacterium *Synechocystis* sp. PCC 6803 to survive rapidly changing light intensities. Plant Physiol **162:** 484–495

Ludwig M, Bryant DA (2012) Acclimation of the global transcriptome of the cyanobacterium *Synechococcus* sp. strain PCC 7002 to nutrient limitations and different nitrogen sources. Front Microbiol **3:** 145

Miyake C, Miyata M, Shinzaki Y, Tomizawa K (2005) CO_2 response of cyclic electron flow around PSI (CEF-PSI) in tobacco leaves: relative electron fluxes through PSI and PSII determine the magnitude of non-photochemical quenching (NPQ) of Chl fluorescence. Plant Cell Physiol **46:** 629–637

Miyake C, Shinzaki Y, Miyata M, Tomizawa K (2004) Enhancement of cyclic electron flow around PSI at high light and its contribution to the induction of non-photochemical quenching of Chl fluorescence in intact leaves of tobacco plants. Plant Cell Physiol **45:** 1426–1433

Munekage Y, Hojo M, Meurer J, Endo T, Tasaka M, Shikanai T (2002) *PGR5* is involved in cyclic electron flow around photosystem I and is essential for photoprotection in *Arabidopsis*. Cell **110:** 361–371

Ohkawa H, Pakrasi HB, Ogawa T (2000) Two types of functionally distinct NAD(P)H dehydrogenases in *Synechocystis* sp. strain PCC6803. J Biol Chem **275:** 31630–31634

Rose RE (1988) The nucleotide sequence of pACYC184. Nucleic Acids Res **16:** 355

Schreiber U, Schliwa U, Bilger W (1986) Continuous recording of photochemical and non-photochemical chlorophyll fluorescence quenching with a new type of modulation fluorometer. Photosynth Res **10:** 51–62

Sejima T, Takagi D, Fukayama H, Makino A, Miyake C (2014) Repetitive short-pulse light mainly inactivates photosystem I in sunflower leaves. Plant Cell Physiol **55:** 1184–1193

Shaku K, Shimakawa G, Hashiguchi M, Miyake C (2015) Reduction-induced suppression of electron flow (RISE) in the photosynthetic electron transport system of *Synechococcus elongatus* PCC 7942. Plant Cell Physiol **57:** 1443–1453

Shimakawa G, Akimoto S, Ueno Y, Wada A, Shaku K, Takahashi Y, Miyake C (2016) Diversity in photosynthetic electron transport under [CO_2]-limitation: the cyanobacterium *Synechococcus* sp. PCC 7002 and green alga *Chlamydomonas reinhardtii* drive an O_2-dependent alternative electron flow and non-photochemical quenching of chlorophyll fluorescence during CO_2-limited photosynthesis. Photosynth Res (in press) 10.1007/s11120-016-0253-y

Shimakawa G, Hasunuma T, Kondo A, Matsuda M, Makino A, Miyake C (2014) Respiration accumulates Calvin cycle intermediates for the rapid start of photosynthesis in *Synechocystis* sp. PCC 6803. Biosci Biotechnol Biochem **78:** 1997–2007

Shimakawa G, Shaku K, Nishi A, Hayashi R, Yamamoto H, Sakamoto K, Makino A, Miyake C (2015) FLAVODIIRON2 and FLAVODIIRON4 proteins mediate an oxygen-dependent alternative electron flow in *Synechocystis* sp. PCC 6803 under CO_2-limited conditions. Plant Physiol **167:** 472–480

Sonoike K (1996) Degradation of *psaB* gene product, the reaction center subunit of photosystem I, is caused during photoinhibition of photosystem I: possible involvement of active oxygen species. Plant Sci **115:** 157–164

Sonoike K (2011) Photoinhibition of photosystem I. Physiol Plant **142:** 56–64

Stevens SE, Porter RD (1980) Transformation in *Agmenellum quadruplicatum*. Proc Natl Acad Sci USA **77:** 6052–6056

Suorsa M, Järvi S, Grieco M, Nurmi M, Pietrzykowska M, Rantala M, Kangasjärvi S, Paakkarinen V, Tikkanen M, Jansson S, et al (2012) PROTON GRADIENT REGULATION5 is essential for proper acclimation of *Arabidopsis* photosystem I to naturally and artificially fluctuating light conditions. Plant Cell **24:** 2934–2948

Takagi D, Takumi S, Hashiguchi M, Sejima T, Miyake C (2016) Superoxide and singlet oxygen produced within the thylakoid membranes both cause photosystem I photoinhibition. Plant Physiol **171:** 1626–1634

Taylor LA, Rose RE (1988) A correction in the nucleotide sequence of the Tn903 kanamycin resistance determinant in pUC4K. Nucleic Acids Res **16:** 358

Trouillard M, Shahbazi M, Moyet L, Rappaport F, Joliot P, Kuntz M, Finazzi G (2012) Kinetic properties and physiological role of the plastoquinone terminal oxidase (PTOX) in a vascular plant. Biochim Biophys Acta **1817:** 2140–2148

van Kooten O, Snel JF (1990) The use of chlorophyll fluorescence nomenclature in plant stress physiology. Photosynth Res **25:** 147–150

Vicente JB, Gomes CM, Wasserfallen A, Teixeira M (2002) Module fusion in an A-type flavoprotein from the cyanobacterium *Synechocystis* condenses a multiple-component pathway in a single polypeptide chain. Biochem Biophys Res Commun **294:** 82–87

Yu L, Zhao J, Muhlenhoff U, Bryant DA, Golbeck JH (1993) PsaE is required for in vivo cyclic electron flow around photosystem I in the cyanobacterium *Synechococcus* sp. PCC 7002. Plant Physiol **103:** 171–180

Zhang P, Allahverdiyeva Y, Eisenhut M, Aro EM (2009) Flavodiiron proteins in oxygenic photosynthetic organisms: photoprotection of photosystem II by Flv2 and Flv4 in *Synechocystis* sp. PCC 6803. PLoS ONE **4:** e5331

Zivcak M, Brestic M, Kunderlikova K, Olsovska K, Allakhverdiev SI (2015a) Effect of photosystem I inactivation on chlorophyll a fluorescence induction in wheat leaves: does activity of photosystem I play any role in OJIP rise? J Photochem Photobiol B **152:** 318–324

Zivcak M, Brestic M, Kunderlikova K, Sytar O, Allakhverdiev SI (2015b) Repetitive light pulse-induced photoinhibition of photosystem I severely affects CO_2 assimilation and photoprotection in wheat leaves. Photosynth Res **126:** 449–463

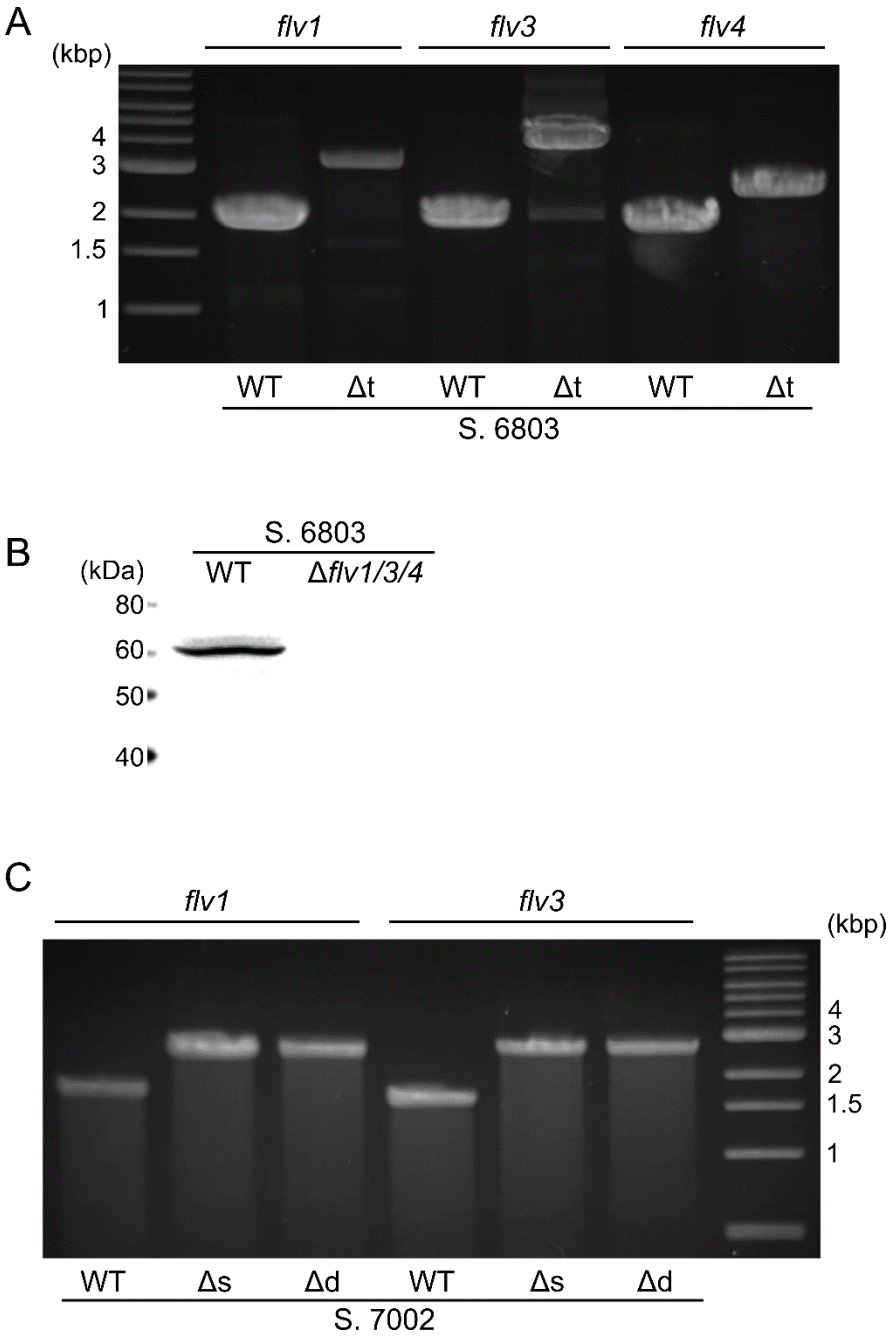

Fig. S1. Insertional inactivation of *flv* genes in S. 6803 and S. 7002. (A) DNA fragments amplified by PCR showing complete segregation of the inactivated genes, *flv1* (*sll1521*) and *flv4* (*sll0217*). WT, S. 6803 WT; Δt, the triple mutant of S. 6803 (Δ*flv1/3/4*). (B) Western blot analysis showing the lack of the *flv3* (*sll0550*) gene product. Extracted soluble fractions (5 µg protein/lane) of S. 6803 WT and Δ*flv1/3/4* were analyzed. (C) DNA fragments amplified by PCR showing complete segregation of the inactivated genes, *flv1* (*SYNPCC7002_A1743*) and *flv3* (*SYNPCC7002_A1321*). WT, S. 7002 WT; Δs, single mutants of S. 7002 (Δ*flv1* and Δ*flv3)*; Δd, the double mutant of S. 7002 (Δ*flv1/3*).

Fig. S1. Shimakawa et al.

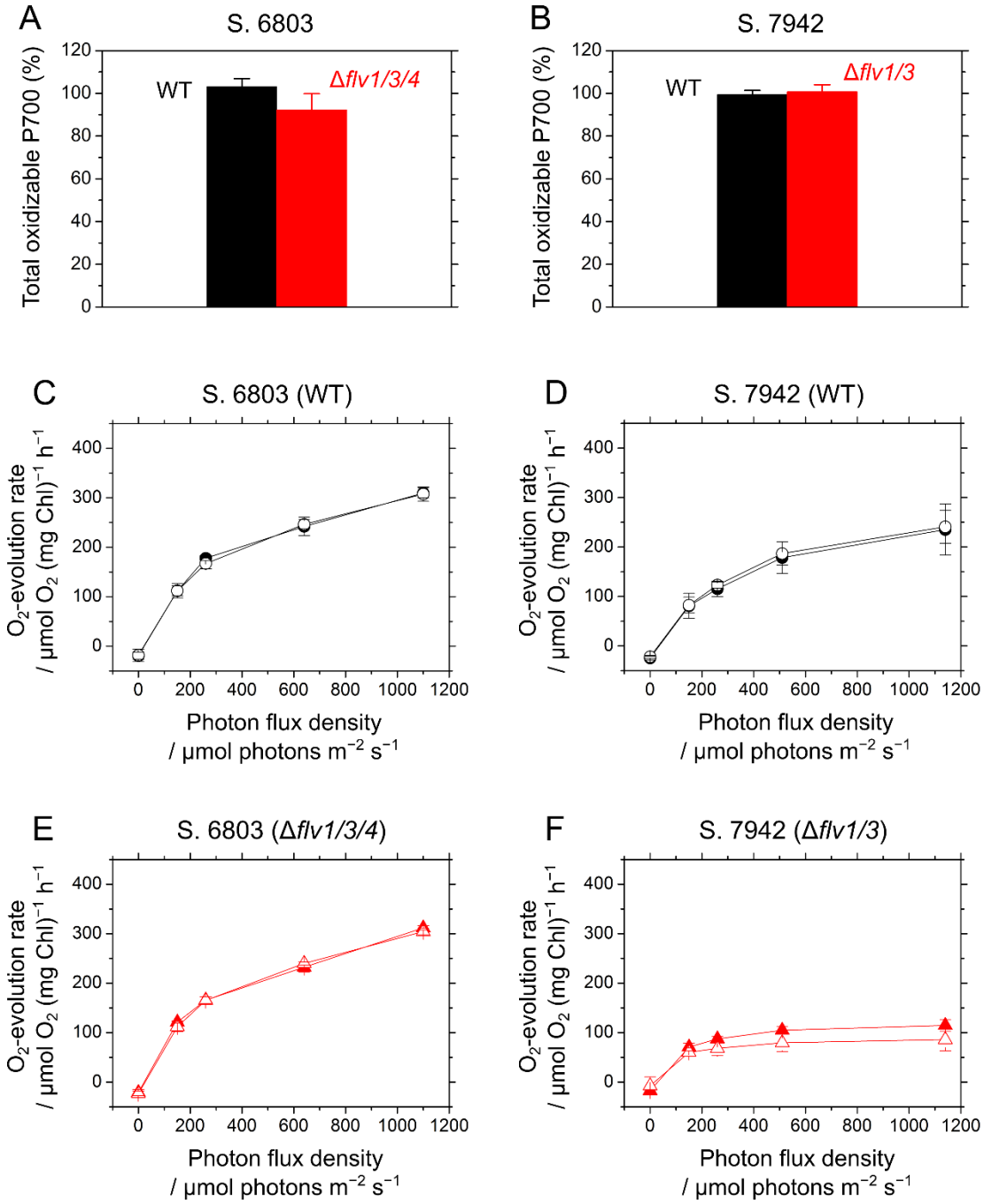

Fig. S2. Decreased activities of PSI and photosynthesis in the WT and the *flv* mutants of S. 6803 (A, C, E) and S. 7942 (B, D, F) after 2-hour exposures to CO_2 limitation during illumination (290 μmol photons m^{-2} s^{-1}). Reaction mixtures contained 50 mM HEPES (pH 7.5) and cells (10 μg Chl mL^{-1}). Residual total oxidizable P700 (A, B) and photosynthetic O_2-evolution rates (C−F) were measured before and after 1 h in the dark following treatments. Black and red symbols represent each WT and *flv* mutant, respectively. Closed and open symbols represent the data before and after the treatments (C−F), respectively. Photosynthetic O_2-evolution rates were measured in the presence of 10 mM $NaHCO_3$. Each measurement was conducted three times, and the means ± SD are shown.

Fig. S2. Shimakawa et al.

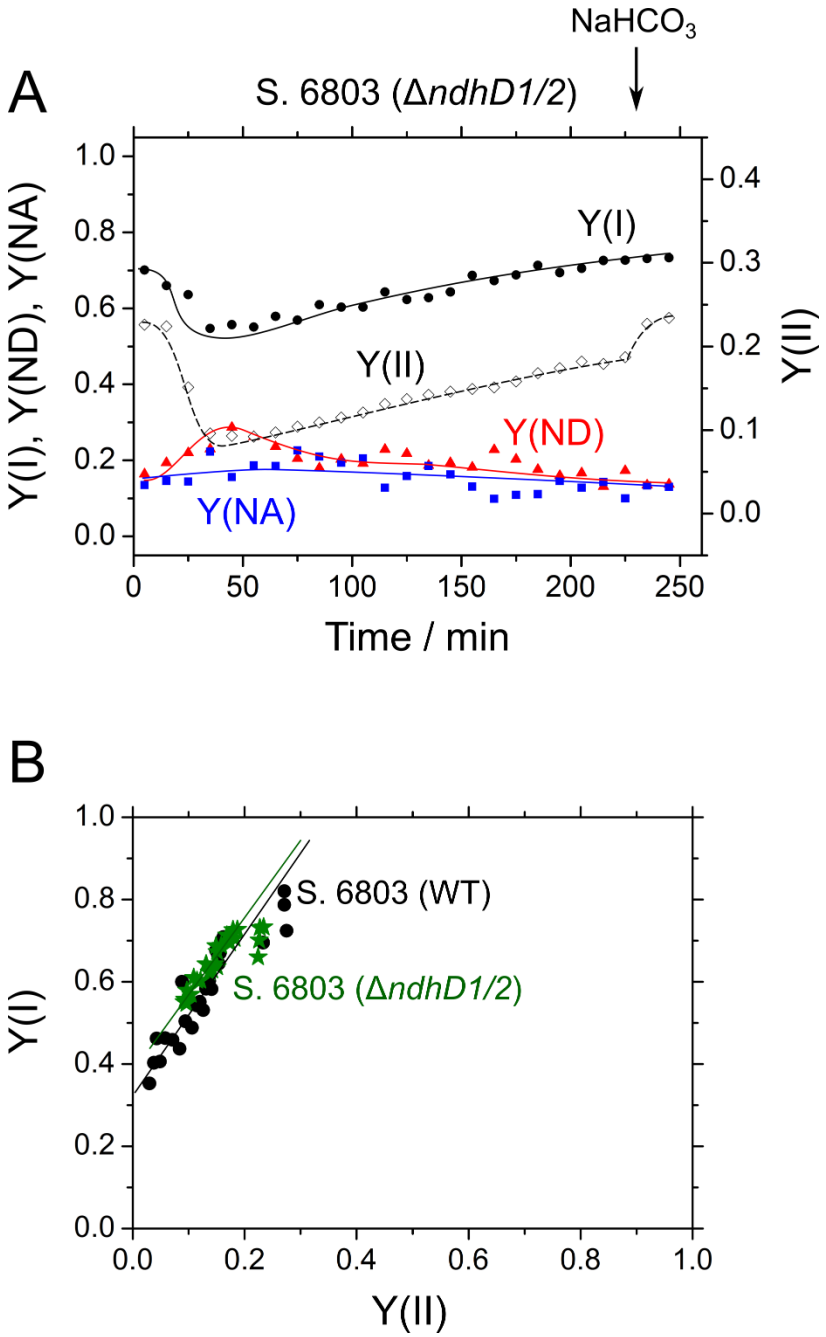

Fig. S3. Responses of the photosynthetic parameters of PSII and PSI to CO_2 limitation in the mutant of S. 6803 deficient in *ndhD1* and *2* (Δ*ndhD1/2*). Reaction mixtures contained the cells (10 µg Chl mL^{-1}). (A) Time courses of the parameters of PSII and PSI. Y(I), black circles; Y(ND), red triangles; Y(NA), blue squares; Y(II), white diamonds. Red AL (180 µmol photons m^{-2} s^{-1}) was activated at time zero. $NaHCO_3$ (10 mM) was added as indicated. Measurements were conducted three times, and representative data are shown. (B) The relationship between Y(II) and Y(I) throughout the measurement in S. 6803 WT (Black circles) and Δ*ndhD1/2* (green stars). Data plotted are obtained from Figs. 3A and S2A, respectively.

Fig. S3. Shimakawa et al.

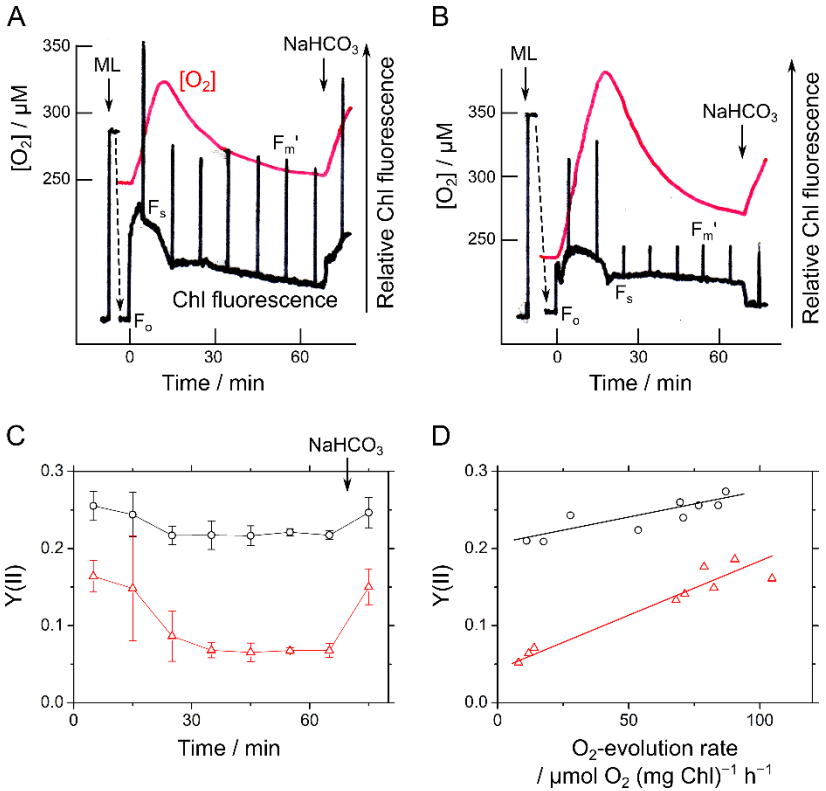

Fig. S4. Photosynthetic parameters of S. 7002 WT and Δ*flv1/3* grown in ambient [CO_2]. (A, B) Time courses of dissolved O_2 concentration (red lines) and relative Chl fluorescence yield (black lines) in S. 7002 WT (A) and Δ*flv1/3* (B). Experimental procedures were similar to those in our recent study (Shimakawa et al., 2016). Cells (10 µg Chl mL^{-1}) were illuminated with measuring light (ML) as indicated. Red AL (300 µmol photons m^{-2} s^{-1}, 620 < λ < 695 nm) was activated at time zero. Dashed arrows indicate changes in the position of the Chl fluorescence signal. Chl fluorescence parameters are: F_o, minimum fluorescence under ML; F_s, steady-state fluorescence under AL; F_m', maximum variable fluorescence under saturating light. $NaHCO_3$ (10 mM) was added as indicated. Experiments were performed three times, and representative data are shown. (C) Time courses of Y(II) shown as mean ± SD (n = 3). Black circles, S. 7002 WT; red triangles, Δ*flv1/3*. (D) Relationships between gross O_2 evolution rates and Y(II) in S. 7002 WT (black circles) and Δ*flv1/3* (red triangles). Photosynthetic O_2 evolution rates were determined at both CO_2-saturated and CO_2-limited conditions in separate experiments (n = 3) following the methods described in Shimakawa et al. (2016).

Fig. S4. Shimakawa et al.

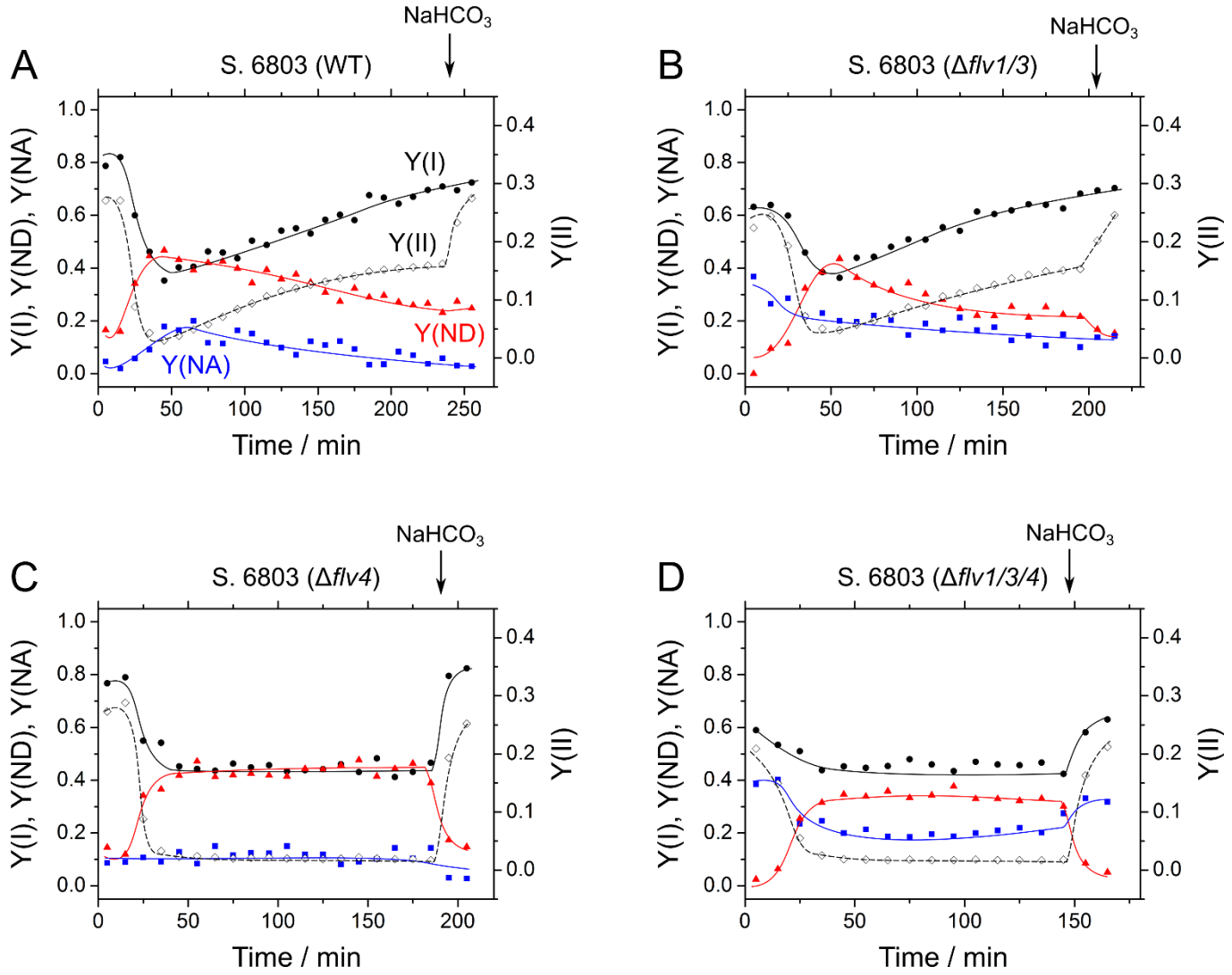

Fig. S5. Responses of the photosynthetic parameters of PSII and PSI to CO_2 limitation in S. 6803 WT (A) and the mutants Δ*flv1/3* (B), Δ*flv4* (C) and Δ*flv1/3/4* (D). Reaction mixtures contained the cells (10 µg Chl mL^{-1}). Y(I), black circles; Y(ND), red triangles; Y(NA), blue squares; Y(II), white diamonds. Red AL (180 µmol photons m^{-2} s^{-1}) was activated at time zero. $NaHCO_3$ (10 mM) was added as indicated. Measurements were conducted three times and representative data are shown.

Fig. S5. Shimakawa et al.

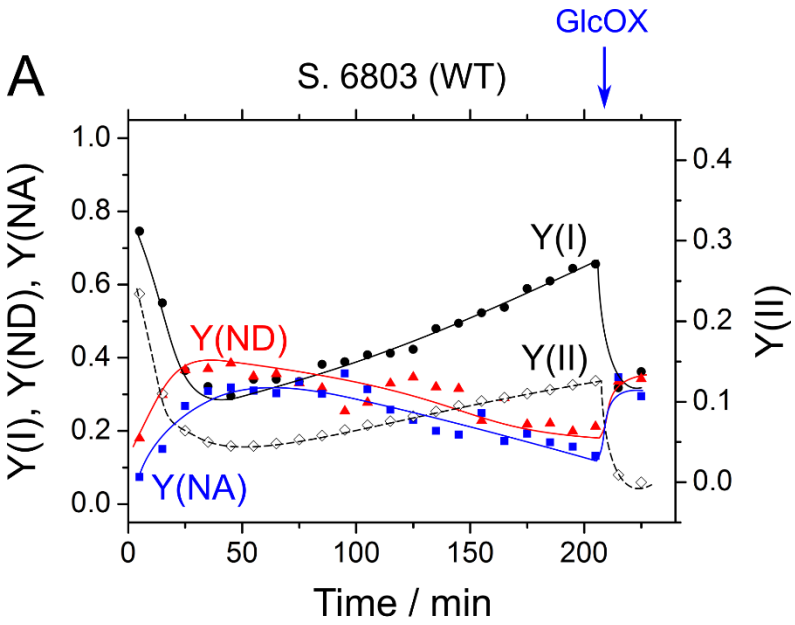

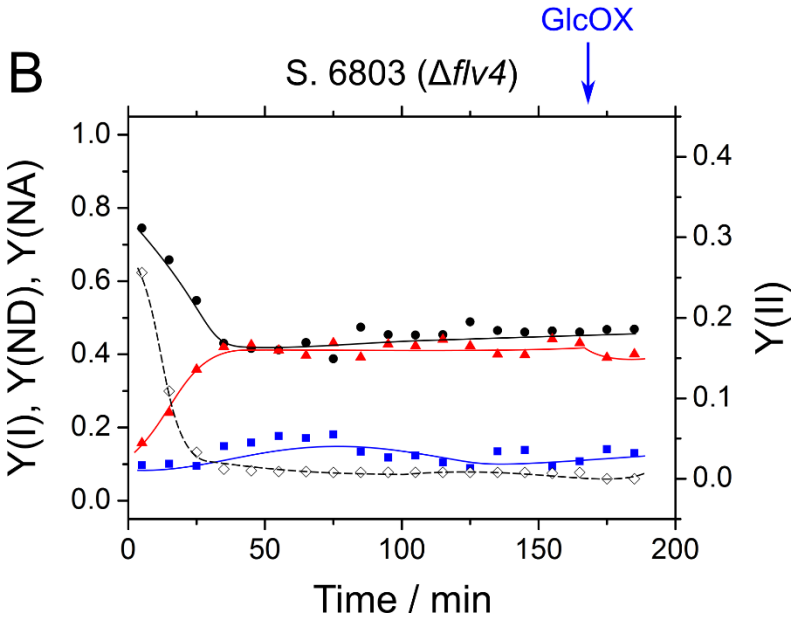

Fig. S6. Effects of eliminating O_2 on the photosynthetic parameters of PSII and PSI under CO_2 limitation in S. 6803 WT (A) and the mutant Δ*flv4* (B). Reaction mixtures contained the cells (10 µg Chl mL^{-1}). Y(I), black circles; Y(ND), red triangles; Y(NA), blue squares; Y(II), white diamonds. Red AL (180 µmol photons m^{-2} s^{-1}) was activated at time zero. Glucose (5 mM), catalase (250 units mL^{-1}), and glucose oxidase (GlcOX, 5 units mL^{-1}) were added as indicated. Measurements were conducted three times and representative data are shown.

Fig. S6. Shimakawa et al.

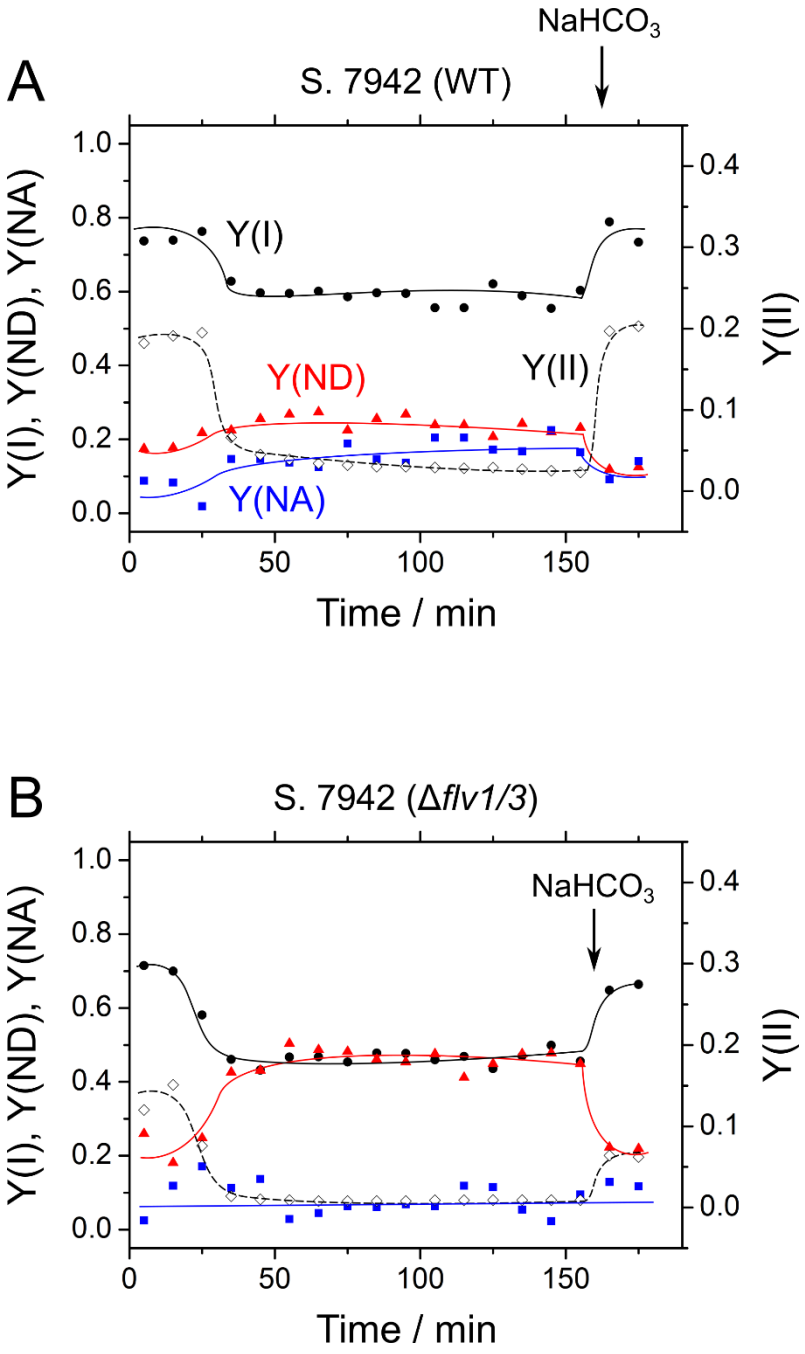

Fig. S7. Responses of the photosynthetic parameters of PSII and PSI to CO_2 limitation in S. 7942 WT (A) and the mutant Δ*flv1/3* (B). Reaction mixtures contained the cells (10 µg Chl mL^{-1}). Y(I), black circles; Y(ND), red triangles; Y(NA), blue squares; Y(II), white diamonds. Red AL (180 µmol photons m^{-2} s^{-1}) was activated at time zero. $NaHCO_3$ (10 mM) was added as indicated. Measurements were conducted three times and representative data are shown.

Fig. S7. Shimakawa et al.

Supplemental Table S1. Primers used in this study

Name	Sequences (5′−3′)
A1743 up f	CTGGGATTCGAAGCACATTTT
A1743 up r	TCTTACGTGCCGATCCGATCCAGTGGCGGTAGTTAT
A1743 dn f	TGACCGTGTGCTTCTACGCTGACCCAGAGGAAATTA
A1743 dn r	GCATAGATCACCCAATGGTCA
A1321 up f	ATCCAGACAGAAAAGGTTAACGAC
A1321 up r	AAACCGCCCAGTCTACCATAATCAGAGACGTAAAATACCG
A1321 dn f	GTTGGGCTTCGGAATGGAGTTGCCGTAGAAATGGTC
A1321 dn r	CGCAGCGACTTTGCTATACAC

1